J Solid State Electrochem (2009) 13:755–762
DOI 10.1007/s10008-008-0604-5

ORIGINAL PAPER

Electrochemical deposition and corrosion stability of Zn–Co alloys

J. B. Bajat · S. Stanković · B. M. Jokić

Received: 29 January 2008 / Revised: 24 April 2008 / Accepted: 28 May 2008 / Published online: 25 June 2008

Abstract Electrochemically deposited Zn–Co alloys under various deposition conditions were investigated using anodic linear sweep voltammetry for phase structure determination, scanning electron microscopy for surface morphology analysis, atomic absorption spectroscopy for determination of chemical composition, and polarization measurements and open circuit potential measurements for determination of corrosion properties. The influence of deposition current density, temperature, and composition of deposition solution on the phase structure and corrosion properties of Zn–Co alloys was studied. It was shown that the ratio of cobalt to zinc ions in the plating bath strongly affects the chemical content and phase structure, as well as corrosion stability, of Zn–Co alloys. Zn–Co alloys deposited from plating baths with the lowest and the highest ratios of cobalt and zinc ions exhibited the lowest corrosion rate.

Keywords Electrodeposition · Zn–Co alloy · ALSV · Phase structure · Corrosion

Introduction

The electrochemical deposition of zinc–cobalt alloys has drawn a lot of attention because these alloys exhibit significantly higher corrosion resistance than pure zinc [1–3]. Furthermore, other properties such as ductility, weldability, hardness, and paintability are also improved. If zinc alloys have effectively high amount of zinc, they can still maintain a sufficiently negative potential to steel and yet, offer better corrosion protection then zinc alone [4]. On the other hand, a higher amount of Co in Zn–Co alloy could provide a barrier type of protection. Due to their properties, Zn–Co alloys are widely used for replacement of zinc on fasteners, appliance and bicycle parts, lighting fixtures, and some hand tools, as well as, furniture, plumbing, and window hardware [5]. As characterized by Brenner [6], the electrodeposition of Zn–Co alloys is considered a codeposition of anomalous type; that is, the less noble component, zinc, deposits preferably with respect to the more noble, cobalt. Because of this fact, the cobalt content in the Zn–Co alloys produced from aqueous plating baths is usually low. Although there are numerous publications regarding Zn–Co alloy with low Co content [3, 7–11], there has not been much work reported on Zn–Co alloys with higher Co content.

The characterization of electrochemically deposited alloys is mostly performed by conventional techniques, such as scanning electron microscopy (SEM), XRD, Auger spectroscopy, etc. However, Despić and coworkers [12–14] have shown that the method of anodic linear sweep voltammetry (ALSV) could also be used for phase structure determination of some alloys. However, no investigation of the relation of Zn alloys phase structure revealed by ALSV and their corrosion stability was reported so far.

It is well known that Zn coatings deposited from baths of various compositions have differences in composition and its homogeneity, porosity, structure, and other characteristics, which, in turn, affect the corrosion resistance of the coatings [1, 15–17]. The aims of this work were to investigate Zn–Co codeposition from a simple plating bath and to find out whether a change in a bath composition could produce alloys with a higher Co content that could offer a better corrosion protection. The plating baths used

J. B. Bajat (✉) · S. Stanković · B. M. Jokić
Faculty of Technology and Metallurgy, University of Belgrade,
P.O. Box 3503, 11120 Belgrade, Serbia
e-mail: jela@tmf.bg.ac.yu

were free of additives since the aim of the work was to investigate only the influence of different cobalt to zinc ratios in the bath. The validity of ALSV technique, giving the opportunity of alloy phase structure determination, was also tested as a simple method of predicting the corrosion stability of alloy deposits obtained.

Experimental

Electrodeposition of Zn–Co alloys

Zn–Co alloys were deposited galvanostatically on a rotating disk electrode (Pt and steel) and steel panel, from chloride baths of the following composition (pH 5.5): 0.1 mol dm^{-3} $ZnCl_2$; 0.4 mol dm^{-3} H_3BO_3; 3 mol dm^{-3} KCl and with a variation of $CoCl_2 \cdot 6H_2O$ concentration from 0.03 to 0.5 mol dm^{-3}. That is, the ratio of $[Co^{2+}/Zn^{2+}]$ in the plating bath was varied and it is given in Table 1. The employed electrolytes were prepared using p.a. chemicals and double distilled water.

The working electrodes were as follows:

(a) Zn–Co alloy deposited on a Pt rotating disk electrode (d=8 mm, at 2,000 rpm) for determining the chemical and phase composition. Prior to each electrodeposition, the Pt disk surface was mechanically polished with a polishing cloth (Buehler Ltd.), impregnated with a water suspension of alumina powder (0.3 μm grade) and then rinsed with pure water in an ultrasonic bath.

The Pt electrode was chosen for chemical content and phase structure determination, since it is an inert substrate and after these measurements it could be clearly seen if the whole Zn–Co deposit was dissolved.

(b) Zn–Co alloy deposited on a steel rotating disk electrode (d=6 mm, at 2,000 rpm) for polarization measurements and on steel panel (20 mm×20 mm× 0.25 mm) for open circuit potential measurements, as well as for SEM and energy dispersive X-ray (EDX) measurements. The steel substrates were pretreated by mechanical cleaning (polishing successively with emery papers of the following grades: 280, 360, 800, and 1,000) and then degreased in a saturated solution of sodium hydroxide in ethanol, pickled with a 1: 1 hydrochloric acid solution for 30 s and finally rinsed with distilled water.

The counter electrodes were as follows:

(a) A zinc spiral ribbon (high purity zinc, surface area 8 cm^2), placed parallel to the RDEs at a distance of 1.5 cm (for plating on a rotating disk electrode), or a zinc panel, placed parallel to a steel panel

Table 1 The ratio of Co^{2+}/Zn^{2+} ions in the plating bath

$[Co^{2+}/Zn^{2+}]$	Bath
0.03/0.1=0.3	A
0.05/0.1=0.5	B
0.1/0.1=1.0	C
0.3/0.1=3.0	D
0.5/0.1=5.0	E

(b) A Pt spiral wire for polarization and corrosion measurements

The reference electrode used in all experiments was a saturated calomel electrode (SCE).

Anodic linear sweep voltammetry

For alloy phase structure determination, alloys were dissolved anodically at room temperature (23±1 °C) using a slow sweep voltammetry technique (sweep rate 1 mV s^{-1} and rotation of 2,000 rpm) in N_2-saturated 0.5 mol dm^{-3} Na_2SO_4+0.05 mol dm^{-3} ethylenediamine tetraacetic acid (EDTA) solution.

Corrosion measurements

The corrosion rates in 3% NaCl solution of the electrodeposited Zn–Co alloys were determined using extrapolation of anodic polarization curves to the open circuit potential. Potential sweep rate of 0.2 mV s^{-1} was applied starting from the open circuit potential (OCP), after the constant OCP was established.

Chemical composition and surface morphology

The chemical composition of the Zn–Co alloys deposited on a Pt electrode was determined by atomic absorption in a AAS-PYE Unicam SP9, Philips.

The surface morphology of different Zn–Co deposits was observed by a JEOL JSM 5800 scanning electron microscope. In order to verify the chemical content of deposited alloys obtained by AAS, chemical analysis was additionally performed for Zn–Co alloys deposited on steel, using an Oxford EDS System connected to the SEM.

Results and discussion

Appearance of deposits

Preliminary experiments were related to deposition of Zn–Co alloys under various deposition conditions (Co^{2+} content in

the plating bath, temperature of the bath, and deposition current density), and based on the appearance of deposits, certain deposition parameters were chosen for further alloy investigation. When deposition was carried out from baths A, C, and E at 5 A dm^{-2}, homogenous and coherent coatings were obtained at 25, 30, and 40 °C. However, for j>10 A dm^{-2} and at higher temperatures (at 30 and 40 °C), deposits appeared less uniform, with rough, powdery deposits. The surface appearance of deposits obtained at low Co concentration (baths A and B) was homogenous and coherent, light gray, but dull. Deposits obtained at higher Co concentrations, especially from baths D and E were gray colored and bright, although deposits obtained from bath D had some very bright spots. So, based on these visual observations, further deposition of Zn–Co alloys was obtained at 25 °C and 5 A dm^{-2}, from different plating baths. All the baths examined had the same concentration of zinc (0.1 mol dm^{-3}), and cobalt concentration in the baths varied from 0.03 mol dm^{-3} (bath A) to 0.5 mol dm^{-3} (bath E).

The structural differences between Zn–Co alloys deposited from different baths can be seen from SEM top view images (×3,000 magnification). SEM analyses of the morphology of the samples studied indicate clear difference between baths used. As an example, Fig. 1a and d shows microphotographs of rather homogenous deposits with different grain sizes, obtained from baths A and E, respectively. The platelet structure of Zn–Co alloy deposit with the smallest amount of Co (1.3 wt.%), shown in Fig. 1a, is very similar to the polycrystalline Zn coating electrodeposited from a sulfate additive-free bath [18]. These microphotographs provide evidence of the increased compactness of these deposits compared to the ones obtained from baths C and D (Fig. 1b and c, respectively). A closer observation of the alloy coatings obtained from baths A and E (Fig. 1a and d) reveals uniform, rather dense and continuous surface coverage, with smaller grain size obtained from bath E.

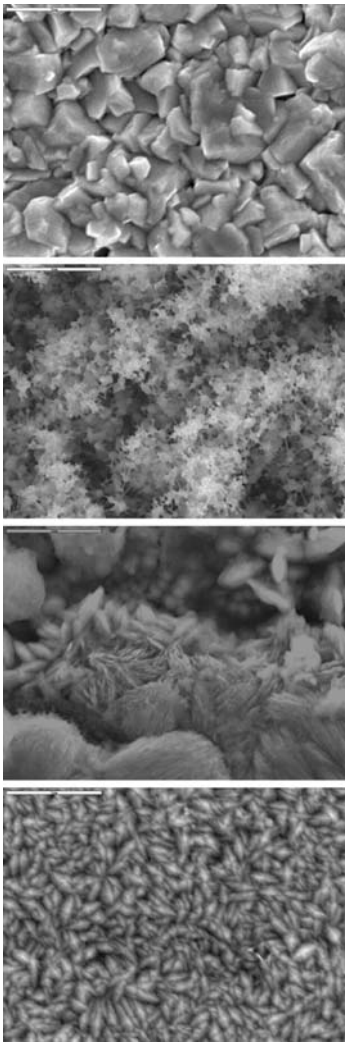

Fig. 1 Surface morphology (SEM) of Zn–Co alloys deposited at 5 A dm^{-2} from baths: **a** A, **b** C, **c** D, and **d** E

Chemical composition of Zn–Co alloys and current efficiency

The Co content in Zn–Co deposits, depending on the ratio of cobalt and zinc ions in the plating bath, was determined by atomic absorption spectrophotometry. Figure 2 illustrates the influence of this ratio on the Co content in the alloy, as well as on the current efficiency.

As can be seen from Fig. 2a, the higher the Co content in the plating bath, the higher the Co content in the deposited alloy. The lowest Co content (1.3 wt.%) was obtained for $[Co^{2+}/Zn^{2+}]$=0.3 (21.3 wt.% Co in the bath, i.e., bath A), and then it gradually increased and reached its maximum of 15.2 wt.% Co for $[Co^{2+}/Zn^{2+}]$=5 (81.9 wt.% Co in the bath, i.e., bath E).

So, it can be concluded that the amount of cobalt deposited strongly depends on the cobalt/zinc ratio in the plating bath. Composition reference line (CRL), representing the ratio of Co^{2+} to total amount of Co^{2+} and Zn^{2+} in the bath [6], is also shown in Fig. 2. Since the Co content in all investigated deposits is below the CRL, it indicates that Zn–Co codeposition follows the anomalous type for all the cobalt/zinc ratios in the bath investigated in this work [6]. That is, lower Co content in Zn–Co alloys is the result of the preferential Zn deposition.

The chemical content given above is the overall content of the Zn–Co alloy deposits. However, deposits obtained from baths C and D were not homogenous, as can be seen from Fig. 1b and c, and local differences in chemical content for these two deposits were determined using EDX. Zn–Co alloy deposit obtained from bath C had 7 wt.% Co, as determined by AAS and shown in Fig. 2a. EDX analysis, though, showed slight differences in the Co content in the

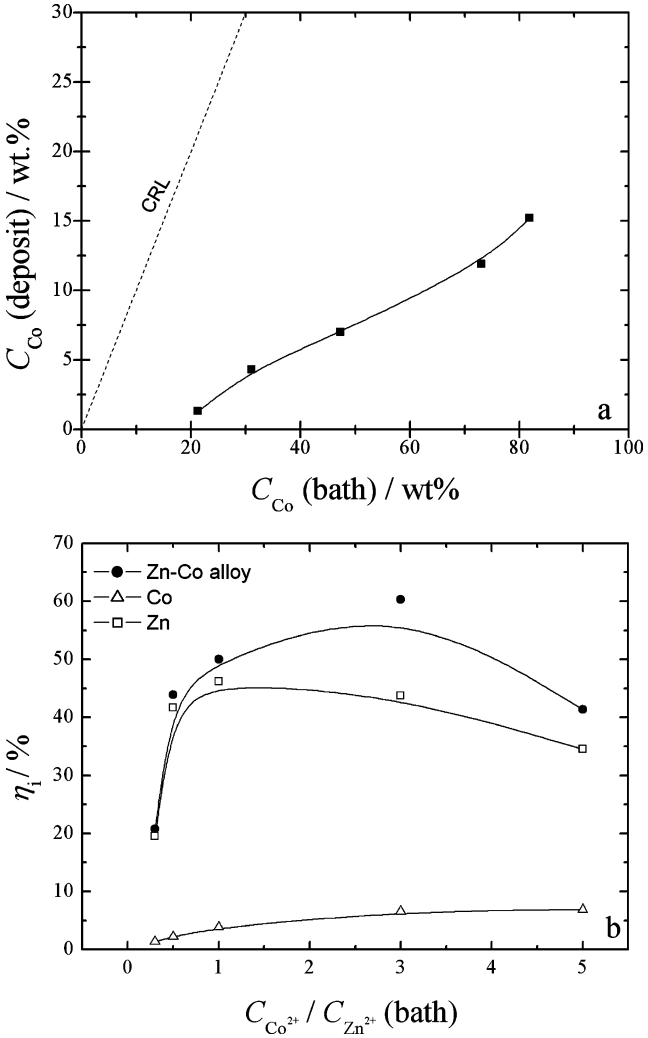

Fig. 2 **a** Variation of Co content in Zn–Co deposits on the Co content in the plating bath. **b** Variation of current efficiencies with ratio of cobalt and zinc ions in the plating bath for Zn, Co, and Zn–Co alloy

different areas of deposit. That is, the black areas in Fig. 1b had 9.5 wt.% Co while the upper white areas had 6.3 wt.% Co. The differences in Co content on different areas, determined by EDX (Fig. 1c), were even more pronounced for Zn–Co alloys deposited from bath D, with Co ranging from 9.9 to 14.25 wt.% Co, whereas the overall chemical content, determined by AAS, was 11.9% Co.

The influence of the ratio of cobalt and zinc ions in the plating bath on the current efficiency (CE, calculated on the basis of the Faradaic law) for Zn, Co, and Zn–Co alloy is shown in Fig. 2b. It could be seen that the current efficiency for Zn deposition is greater than CE for Co deposition for all investigated Co^{2+}/Zn^{2+} ratios. In addition, the CE for alloy plating is below 60% for all Co^{2+}/Zn^{2+} ratios. It should be noted that CE for cobalt deposition increases gradually with the increase of Co^{2+}/Zn^{2+} ratio in the bath. However, zinc and alloy CE increase sharply, reach a maximum, and then decrease. Similar results were reported in literature [19] for Zn–Co alloy deposition from sulfate plating bath.

The effect of Co concentration in the plating bath on the alloy deposition

Galvanostatic curves for deposition of Zn–Co alloys from plating baths with different ratios of Co and Zn ions are represented in Fig. 3. It could be seen that the deposition potential greatly depends on the ratio of Co and Zn ions in the plating bath. That is, Zn–Co alloy deposited mainly at −1.32 V from a bath with the lowest amount of Co in the bath (bath A) and deposition potentials gradually advanced to more noble values as the concentration of Co in the bath increased. According to Fig. 3, lower overpotential is needed to create initial nucleus during deposition from baths with higher Co^{2+} content. Similar results were reported for Zn–Ni deposition [2]. The little potential shivering in the galvanostatic curves, especially pronounced for curve related to Zn–Co deposition from bath A, is the result of the hydrogen evolution and, as suggested by Yan et al. [20], could also be associated to the formation of small amounts of ZnO during electrodeposition, although it was not detected by EDX. This is in agreement with the results presented in Fig. 2b, where it was shown that the lowest current efficiency is for Zn–Co deposition from bath A ($[Co^{2+}/Zn^{2+}]=0.3$), meaning that hydrogen evolution, which is a parallel reaction taking place on a cathode, is the highest in the case of deposition from bath A.

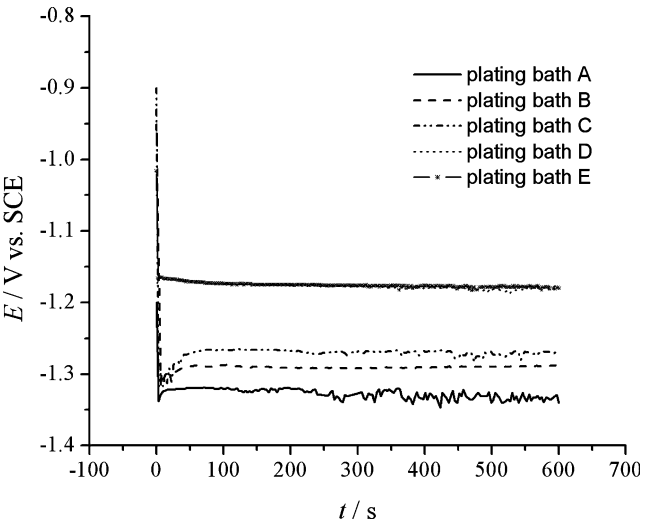

Fig. 3 Galvanostatic curves at 5 A dm^{-2} for deposition of Zn–Co alloys from plating baths with different ratios of cobalt and zinc ions

The influence of concentration of Co ions in the plating bath on alloy phase structure: ALSV measurements

When an alloy film is polarized anodically under potentiodynamic conditions, the components will dissolve at various potentials, depending on their equilibrium and kinetic properties. When the activity of the component in a phase reduces to zero, the dissolution current peak will be produced. Various phase structures and chemical forms present in the alloy will produce various current peaks. Therefore, the peak structure obtained is the characteristics of the alloy components and phase structure of the deposit [21]. Very important results concerning the Zn–Ni alloy deposition and phase characterization were published by Swathirajan [17, 22].

The main problem in the use of this technique is finding a suitable electrolyte in which the electrodeposited material would dissolve gradually and thoroughly. Alloy phase structure was investigated by anodic linear sweep voltammetry in Na_2SO_4 solution containing complex forming ions, in the presence of which Zn–Co alloy completely dissolves. That is, it is well known that pure Zn dissolves and zinc alloys do not dissolve in Na_2SO_4 solution, while in the presence of a small amount of complex forming agents (EDTA) both Zn and its alloys dissolve [21].

Figure 4 represents ALSV voltammograms of Zn–Co deposits of different thicknesses. This experiment was carried out in order to establish the dependence of ALSV on the thickness of the deposit (expressed by the time of the electrodeposition) and to determine whether the entire quantity of the alloy is dissolved during the sweep of potential across the range covered by the corresponding peak. It is seen that the peak heights depend on the thickness of the deposited layer, but the number of peaks and peak potentials remain the same, regardless of the thickness. This indicates the stability of the phase structures obtained. Furthermore, the charge under the current peaks is proportional to the thickness of the deposit indicating that the entire thin film is dissolved during the potential sweep. It was also found that the Faradaic efficiency of the peaks was constant.

Since it was shown that the number of phases determined by ALSV does not depend on the thickness of deposited coatings, the thickness of 5 μm was chosen for further work.

The concentration of Co ions in the plating bath has a significant influence on the voltammograms, i.e., the alloy phase structure. As can be seen from Fig. 5a, the increase of the Co content in the plating bath favors the formation of new phases. That is, there is only one current peak, at about −0.800 V (peak I in Fig. 5a), for Zn–Co alloy deposited from a bath with the lowest concentration of Co (bath A). The increase of the Co concentration in the bath from 0.03 mol dm^{-3} (bath A) to 0.05 mol dm^{-3} (bath B) gives rise to three current peaks (I, II, and III in Fig. 5a),

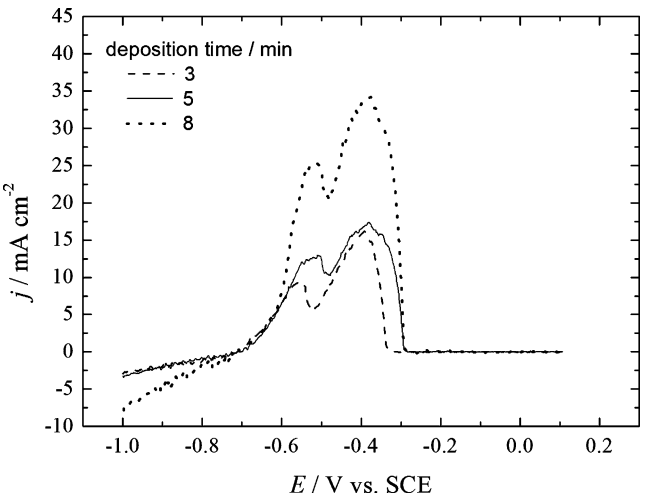

Fig. 4 ALSV voltammograms in Na_2SO_4 + EDTA solution of dissolution of Zn–Co alloy deposited during different time duration (3, 5, and 8 min) from bath D, at 5 A dm^{-2}, ω=2,000 rpm, υ=1 mV s^{-1}

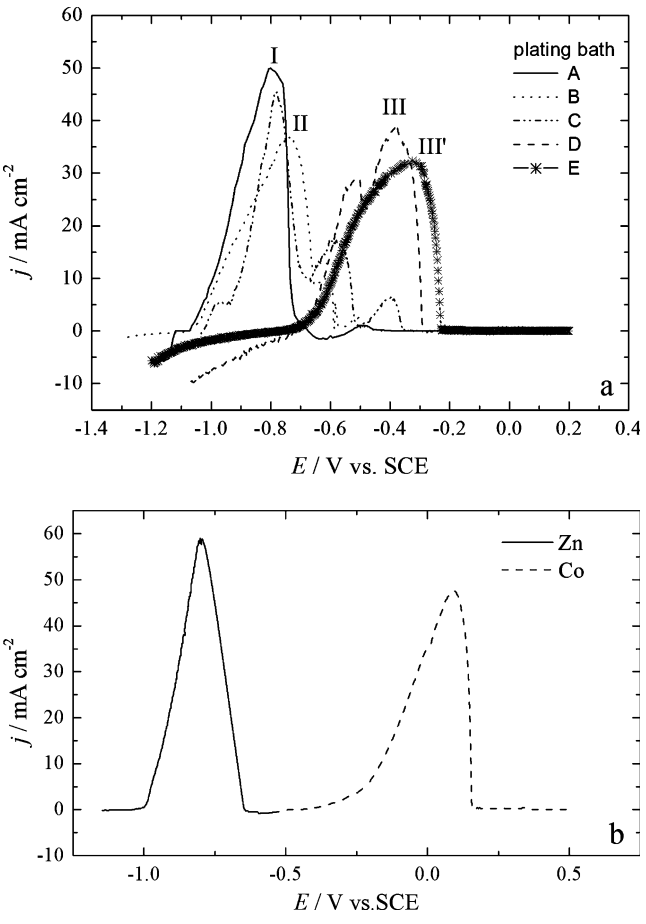

Fig. 5 **a** ALSV voltammograms in Na_2SO_4 + EDTA solution of dissolution of Zn–Co alloys (5 μm thickness) deposited from plating baths with different ratios of cobalt and zinc ions at 5 A dm^{-2}, ω=2,000 rpm, υ=1 mV s^{-1}. **b** ALSV voltammograms in Na_2SO_4 + EDTA solution of dissolution of Zn and Co, ω=2,000 rpm, υ=1 mV s^{-1}

which are much better resolved when the concentration of Co in the plating bath is further increased to 0.1 mol dm^{-3} (bath C). However, the additional increase of Co content in the plating bath to 0.3 mol dm^{-3} (bath D) and 0.5 mol dm^{-3} (bath E) results with a decrease in the number of current peaks, so two phases are present when Zn–Co alloy is deposited from bath D and only one phase when depositing from a plating bath with the highest amount of Co (bath E). Dissolution peaks of deposits obtained from the plating bath with low Co content in the bath (bath A) were close to the dissolution peak of pure Zn (Fig. 5b). The peak potentials gradually shift to more noble values, towards Co dissolution peak (Fig. 5b) as the concentration of Co in the bath increases to 0.5 mol dm^{-3} (bath E), indicating that different phases of Zn–Co alloys (with higher Co content) are obtained by deposition from plating baths with different ratios of alloying metals in the bath.

On the basis of ALSVs, chemical composition and equilibrium phase diagram [23], as well as on the data reported by other authors for Zn–Co alloys of similar characteristics and obtained by similar deposition parameters [24, 25], it is supposed that the dissolution peak at −0.800 V is mainly due to the preferential dissolution of Zn from Zn–Co solid solution. The dissolution potential of peak I is close to the dissolution potential of pure Zn (Fig. 5b), while other peaks correspond to the dissolution of phases richer in Co. As the Co content in the alloy increases (Fig. 5a), the potentials of these later peaks shift to more noble values, closer to the potentials of pure Co dissolution (Fig. 5b).

Corrosion stability

In order to determine corrosion stability, the plated specimens (10 μm thickness) were immersed in a 3% aqueous NaCl solution, and the open circuit potential (E_{ocp}) was measured daily. Figure 6 shows the time dependence of E_{ocp} for steel plated by Zn–Co alloys deposited from different plating baths. The open circuit potential of bare steel surface in 3% NaCl was −640 mV vs. SCE and it is marked with a line in Fig. 6. The potentials of the Zn–Co alloys are more negative than E_{ocp} of steel base, so Zn–Co deposits offer sacrificial cathodic protection. The E_{ocp} values of steel modified by Zn–Co alloys increase positively with time of immersion and reach the steel E_{ocp}, which represents loss of the deposit and the start of a corrosion process. The open circuit potentials of alloys deposited at the same current densities from different plating baths differ initially but eventually reach almost the same values. The initial E_{ocp} difference is due to the alloy phase difference and the difference in the chemical composition. The Zn–Co alloys deposited from baths A and B are rich in Zn (Figs. 2 and 5) and thus the initial E_{ocp} of this alloy is close to the E_{ocp} of zinc (−1.055 V; Table 2).

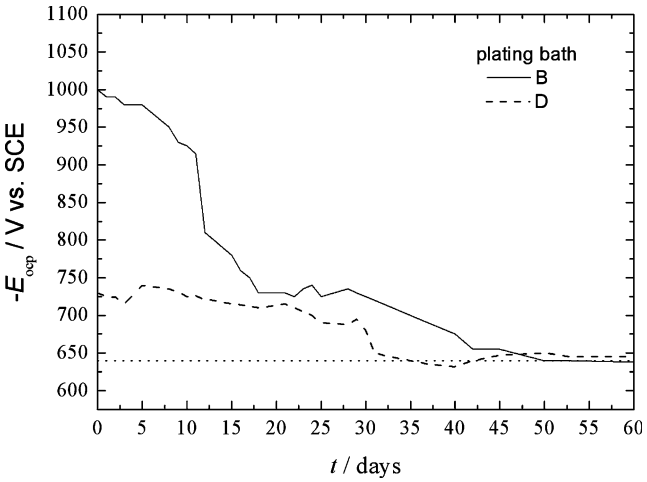

Fig. 6 The dependence of E_{ocp} for Zn–Co alloys deposited on steel from baths B and D at 5 A dm^{-2} (10 μm thickness)

The E_{ocp} of Zn–Co alloys obtained from plating baths D and E, however, lie somewhere between the open circuit potentials of pure Zn and pure Co, since these alloys do not have a Zn-rich phase (Figs. 2 and 5). The results of the visually observed alloy destruction in 3% NaCl solution, or the appearance of red rust on the steel base, are presented in Table 2. The longest time to rest rust appearance, indicating the best corrosion stability, was observed for Zn–Co alloy deposited from plating baths A and E.

Anodic polarization curves in a small range of potential near OCP were obtained in a 3% NaCl solution. Some of the E−log j dependences obtained are shown in Fig. 7. The corrosion current densities, j_{corr}, were estimated from the intersections of the anodic Tafel plots with the OCP. The corrosion potentials, E_{corr}, and the corresponding corrosion currents for the alloy samples are given in Table 2. Data in Table 2 are the mean values of three to five measurements.

As can be seen from Table 2, corrosion current densities gradually increase with the increase of the $[Co^{2+}/Zn^{2+}]$ ratio in the plating bath, reach a maximum, and then drop. The lowest corrosion rate was observed for the Zn–Co alloy deposited from the solution with the smallest $[Co^{2+}/Zn^{2+}]$ ratio, i.e., coating containing small amounts of Co, 1.3 wt.%

Table 2 The time of red rust appearance, corrosion potentials, E_{corr}, and corrosion current densities, j_{corr}, for Zn–Co alloys deposited from different plating baths

Bath	Time/days	$-E_{corr}$, V vs. SCE	j_{corr}, μA cm^{-2}
A	55	1.010	11
B	50	1.000	27
C	47	0.985	39
D	35	0.730	50
E	52	0.720	20

Data are mean values of three to five measurements.

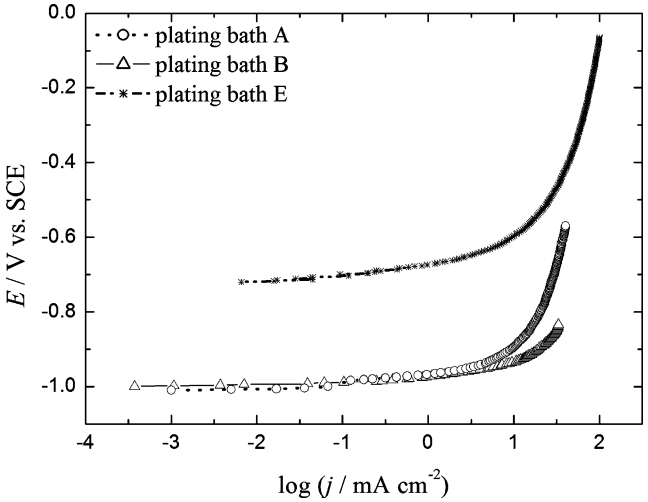

Fig. 7 Anodic polarization curves in 3% NaCl for Zn–Co alloys deposited from plating baths with different ratios of cobalt and zinc ions (A, B, E) at 5 A dm^{-2} (ω=2,000 rpm, υ=0.2 mV s^{-1})

(bath A), as well as the one with the greatest [Co^{2+}/Zn^{2+}] ratio, i.e., coating containing 15.2 wt.% Co (bath E). Similar results were reported by Short and coworkers [26] who showed that the lowest corrosion rates of Zn–Co alloys, with Co ranging from 0.5% to 19.9%, were when the amount of Co was 1% and 10%. This is most probably due to the most uniform distribution of cobalt, as the alloying element, in the zinc crystal lattice.

Chemical analysis showed that alloys deposited from baths with higher [Co^{2+}/Zn^{2+}] ratio (baths B and C) have greater Co content (Fig. 2a). These alloys also have more phases present in the deposit (Fig. 5a). The reduced protective properties of Zn–Co alloys deposited from baths B and C could be due to the formation of three phases (denoted by three different voltammetric peaks, i.e., I, II, and III in Fig. 5a), since the multiphase systems could lead to galvanic coupling of the deposit. However, a further increase of [Co^{2+}/Zn^{2+}] ratio in the bath (bath D) results in further increase of Co content in the alloy (i.e., 11.9 wt.% Co), corrosion current density is also increased, and time to red rust appearance reduced (Table 2). This clearly indicates the reduced protective properties of deposits obtained from bath D, and it is probably due to the dual phases obtained (Fig. 5a). When [Co^{2+}/Zn^{2+}] ratio in the bath is additionally increased (bath E), the protective properties of Zn–Co deposits are improved again, i.e., corrosion current density decreases and time to red rust appearance increases (Table 2). This could be explained by the formation of the solid solution of Co in Zn, consisting of only one phase structure, which is characterized by peak potential III′ in Fig. 5a.

It should be noted that there are only small amounts of phases corresponding to dissolution peaks II and III in deposits obtained from plating baths B and C, and a larger amount of phase II in the deposit obtained from plating bath D (Fig. 5a). To be exact, the amount of phase II (calculated by the charge under the corresponding dissolution peak) related to dissolution of Zn–Co alloy obtained from bath D is 1.5 times larger than the overall amount of phases II and III related to dissolution of Zn–Co alloy obtained from bath C and more than five times larger than the overall amount of phases II and III related to dissolution of Zn–Co alloy obtained from bath B.

On the basis of all the results presented, it could be concluded that a small amount of Co in the alloy (1.3 wt.%) results in the formation of a single phase Zn–Co alloy which provides sufficient corrosion protection. An increase of Co in the alloy deposit (above 1.3 wt.%) leads to the formation of new alloy phases, which result to reduced corrosion properties. However, a further increase of Co to 15.2 wt.% in alloy deposits leads to deposition of a single phase alloy again, which results with better protective properties. So, it could be concluded that a single phase Zn–Co alloy would have better corrosion stability in respect to a multiphase alloy deposit. Zn–Co alloys deposited from plating baths A and E showed the best corrosion stability, i.e., the longest time to red rust appearance, as well as smaller j_{corr}.

So, it could be concluded that the ALSV technique, giving the opportunity of the alloy phase structure determination, showed to be a simple method of predicting the corrosion stability of alloy deposits obtained.

Conclusion

On the basis of the results presented, it could be concluded that a ratio of cobalt to zinc ions in the plating bath has a significant influence on the chemical composition, current efficiency, phase structures formed, as well as on the corrosion stability of Zn–Co electrodeposited alloys.

Different phases of Zn–Co alloys obtained by electrochemical deposition were verified by anodic linear sweep voltammetry. The ALSV technique, giving the opportunity of alloy phase structure determination, was shown as a simple method of predicting the corrosion stability of alloy deposits obtained. That is, single-phased Zn–Co alloys (as revealed by ALSV) deposited from plating baths A and E showed the best corrosion stability, i.e., the longest time to red rust appearance, as well as smaller j_{corr}. On the other hand, deposits with intermediate Co content were formed with more phases, as determined by ALSV, and it is proposed that their presence is the cause for galvanic coupling and thus, the increased corrosion of alloy deposits.

So, based on the ALSV measurements (number of peaks, their potentials, as well as charge under peaks), it is possible to anticipate the phases present in the alloy deposit, as well as its corrosion stability.

Acknowledgment This research was financed by the Ministry of Science and Environmental Protection, Republic of Serbia, contract no. 142061.

References

1. Pushpavanam M, Natarajan SR, Balakrishnan K, Sharma LR (1991) J Appl Electrochem 21:642
2. Abou-Krisha MM, Assaf FH, Toghan AA (2007) J Solid State Electrochem 11:244
3. Chen PY, Sun IW (2001) Electrochim Acta 46:1169
4. Pech-Canul MA, Ramanauskas R, Maldonado L (1997) Electrochim Acta 42:255
5. Lay DE, Eckles WE (1990) Plating Surf Finish 9:10
6. Brenner A (1963) Electrodeposition of alloys, vol. 2. Academic, New York, p 194
7. Boshkov N, Petrov K, Kovacheva D, Vitkova S, Nemska S (2005) Electrochim Acta 51:77
8. Ramanauskas R, Muleshkova L, Maldonado L, Dobrovolskis P (1998) Corros Sci 40:401
9. Ramanauskas R, Juskenas R, Kalinicenko A, Darfias-Mesias LF (2004) J Solid State Electrochem 8:416
10. Boshkov N, Petrov K, Vitkova S, Nemska S, Raichevsky G (2002) Surf Coat Technol 157:171
11. Bajat JB, Mišković-Stanković VB, Maksimović MD, Dražić DM, Zec S (2002) Electrochim Acta 47:4101
12. Despić A, Jović V (1995) In: White RE et al (ed) Modern aspects of electrochemistry, vol. 27. Plenum, New York, pp 143
13. Stevanović JS, Jović VD, Despić AR (1993) J Electroanal Chem 349:365
14. Stevanović J, Skibina L, Stefanović M, Despić A, Jović V (1992) J Appl Electrochem 22:172
15. Srivastava RD, Mukerjee RC (1976) J Appl Electrochem 6:321
16. Elkhatabi F, Benballa M, Sarret M, Muller C (1999) Electrochim Acta 44:1645
17. Swathirajan S (1986) J Electrochem Soc 133:671
18. Li MC, Jiang LL, Zhang WQ, Qian YH, Luo SZ, Shen JN (2007) J Solid State Electrochem 11:1319
19. Prasad KA, Giridhar P, Ravindran V, Muralidharan VS (2001) J Solid State Electrochem 6:63
20. Yan H, Downes J, Boden PJ, Harris SJ (1996) J Electrochem Soc 143:1577
21. Bajat JB, Maksimović MD, Radović GR (2002) J Serb Chem Soc 67:625
22. Swathirajan S (1987) J Electroanal Chem 221:211
23. American Society for Metals (1973) Metals handbook: metallography, structures and phase diagrams, vol. 8. American Society for Metals, Ohio, p 290
24. Karwas C, Hepel T (1989) J Electrochem Soc 136:1672
25. Gomez E, Alcobe X, Valles E (2001) J Electroanal Chem 505:54
26. Short NR, Abibsi A, Dennis JK (1989) Trans Inst Met Finish 67:73